Electronic Supplementary Material (ESI) for Physical Chemistry Chemical Physics.


*Supplementary information*

# A new insight for ohmic contacts to $MoS_2$: by tuning $MoS_2$ affinity energies but not metal work-functions

**Qian Wang,[1,2] Bei Deng,[2] and Xingqiang Shi[2,*]**

[1]*Harbin Institute of Technology, Harbin 150080, China*

[2]*Department of Physics, South University of Science and Technology of China, Shenzhen 518055, China*

*E-mail: shixq@sustc.edu.cn

**Contents:**

## Section 1. P-type SBH for $MoS_2$/Pt

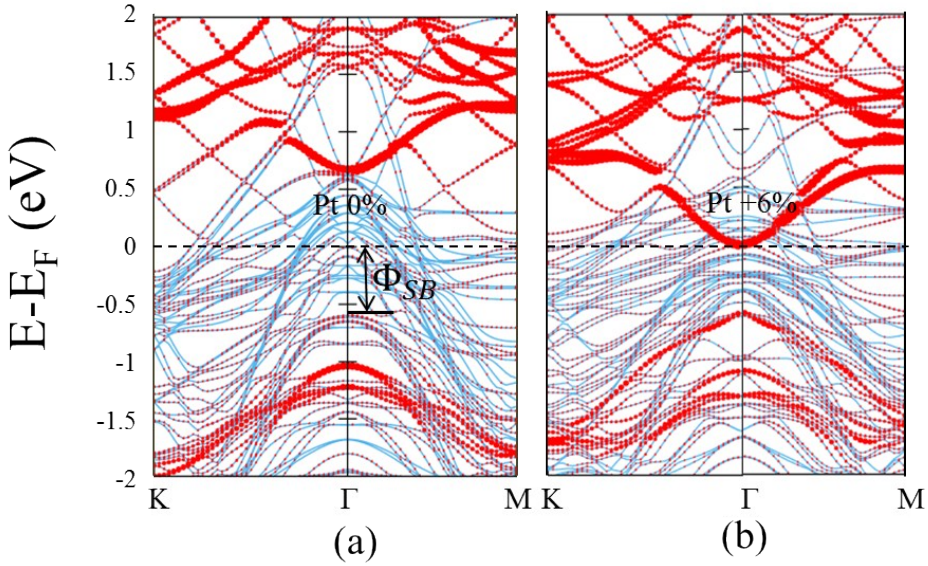


Fig. S1 Band structures of single-layer $MoS_2$ in contacted with Pt (111) surfaces without and with 6% strain. The blue curves are the overall band structures. The red dots represent the projection of Mo *d*-orbitals with its weight represented by the dot size. The Fermi level is set at zero, as shown by the black dotted line.

The projected band structure of single-layer $MoS_2$ in $MoS_2$/Pt surface without strains is shown in Fig. S1 (a). The Schottky barrier (SB) in this contact belongs to p-type. The p-type SB is defined as the energy difference between the valence band maximum (VBM) and $E_F$. So the p-type $\Phi_{SB}$ can be defined as:

$$\Phi_{SB} = IE_{MoS2}^{S/M} - E_F \tag{1}$$

where $E_F$ is the Fermi level in $MoS_2$/metal system and $IE_{MoS2}^{S/M}$ is the ionization energy of $MoS_2$ in $MoS_2$/metal. Both $E_F$ and $IE_{MoS2}^{S/M}$ are defined as relative to the vacuum level.

In the Schottky-Mott mode, the p-type SB is given by the difference between the work function of metal, $W_M$, and the ionization energy of the single layer $MoS_2$, $IE_{MoS_2}$. Neglecting the interaction between metal and semiconductor, the SBH should ideally follow the predictions of the formula:

$$\Phi_p = IE_{MoS_2} - W_M \tag{2}$$

where $\Phi_p$ is the Schottky barrier height (SBH) caluculted by Schottky-Mott model.

Considering interface diople ΔV, SBH can be calculated by modified Schottky-Mott model and shown as:

$$\Phi_{pm} = IE_{MoS_2} - W_M + \Delta V \tag{3}$$

where $\Phi_{pm}$ is SBH calculated by modified Schottky-Mott model method.

The SB in $MoS_2$/Pt without strain is p-type and the value of SBH is 0.65 eV shown in Fig. S1(a). However, the p-type SB transforms to n-type with tensile strain, and the value turn to 0 eV with 6% strain.

## Section 2. The partial density of states of Mo atoms in $MoS_2$/Pd, $MoS_2$/Pt, and $MoS_2$/Au contacts

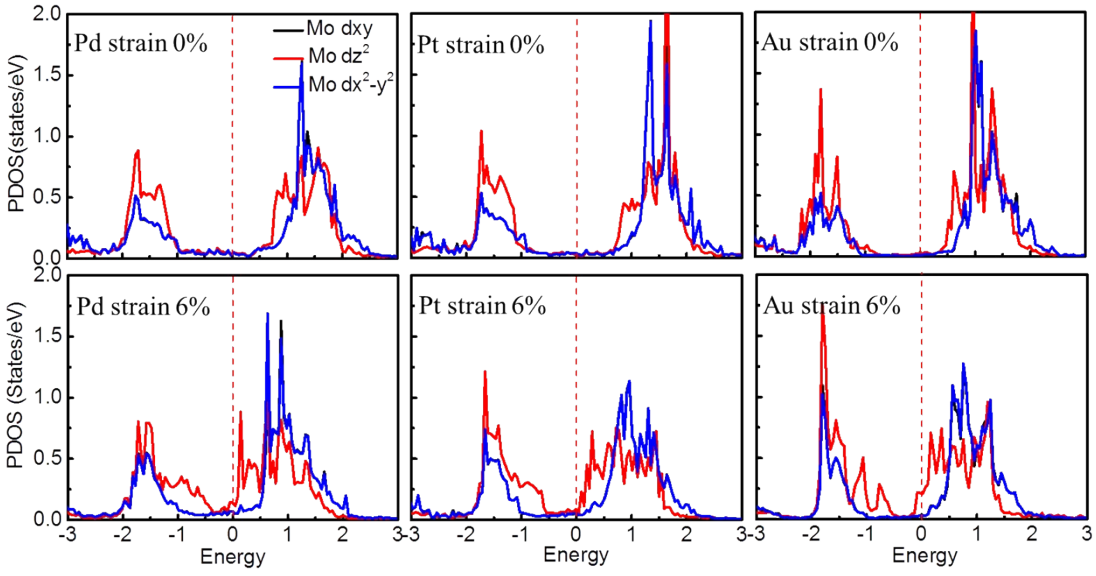


Fig. S2 Partial density of states (PDOS) of *d* orbitals of Mo atoms in $MoS_2$/Pd, $MoS_2$/Pt, and $MoS_2$/Au. The red vertical dash lines represent the Fermi level.

Fig. S2 shows the partial density of states (PDOS) of *d* orbitals of Mo atoms in the $MoS_2$/Pd, $MoS_2$/Pt, and $MoS_2$/Au configurations under 0% and 6% strain, respectively. The total density of

states of the $MoS_2$ layer is dominated by the *d* orbitals of Mo atoms near the Fermi level, as discussed in the main text. Therefore, the Mo atoms have an important influence on the SBH.

The conduction band part of Mo atoms near the Fermi level is mainly dominated by the $d_{z2}$, $d_{xy}$ and $d_{x2-y2}$ orbitals of Mo atoms,[1] as demonstrated in Fig. S2. The sharp red peaks above the Fermi level, illustrates that the $d_{z2}$ orbitals dominate the CBm state. Obviously, with the the effect of strain, the energy separation between CBm and Fermi level is reduced to 0. This means that SBHs in $MoS_2$/Pd, $MoS_2$/Pt, and $MoS_2$/Au are turn to zero with ~6% tensile strain or lower, which is consistent with the conclusions from the band structure of Fig. 2 in the main text.

## Section 3. The variation of electron affinity χ and ionization energy IE of single-layer TMDCs with strain

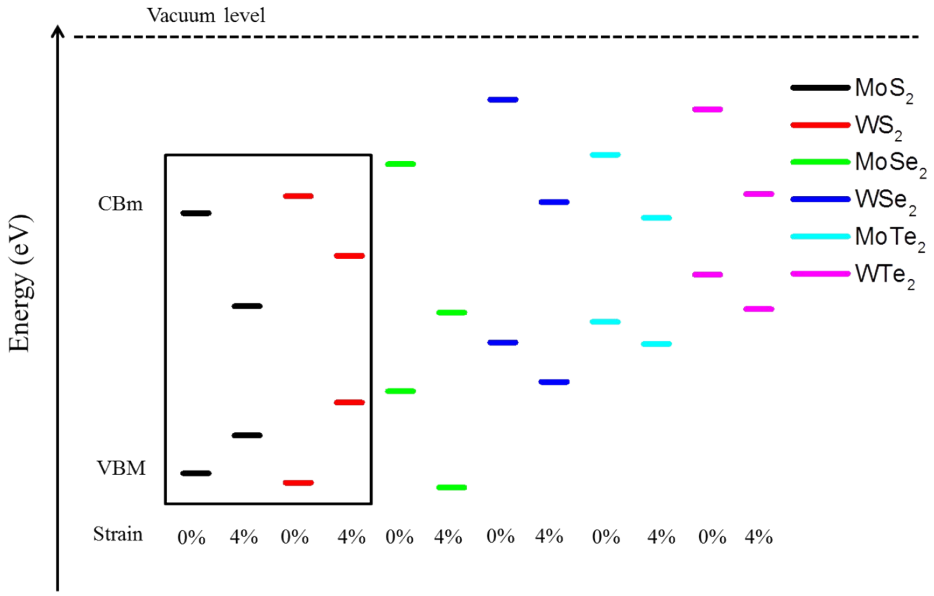


Fig. S3. The energy level alignment with strain of electron affinity $\chi$ (CBm) and ionization energy $IE$ (VBM) of single-layer TMDCs, including $MoS_2$, $WS_2$, $MoSe_2$, $WSe_2$, $MoTe_2$ and $WTe_2$. The energy reference is the vacuum level.

Table S1. Values of electron affinity $\chi$ (CBm) and ionization energy $IE$ (VBM) of single-layer TMDs in $MoS_2$,$WS_2$, $MoSe_2$, $WSe_2$, $MoTe_2$ and $WTe_2$ with strain.

| strain | 0% | 4% |
|---|---|---|
| $MoS_2$ $\chi$ | 4.59 | 5.18 |
| $MoS_2$ $IE$ | 6.24 | 6.00 |
| $WS_2$ $\chi$ | 4.48 | 4.86 |
| $WS_2$ $IE$ | 6.30 | 5.79 |
| $MoSe_2$ $\chi$ | 4.28 | 5.22 |
| $MoSe_2$ $IE$ | 5.72 | 6.33 |
| $WSe_2$ $\chi$ | 3.87 | 4.52 |
| $WSe_2$ $IE$ | 5.41 | 5.66 |
| $MoTe_2$ $\chi$ | 4.22 | 4.62 |
| $MoTe_2$ $IE$ | 5.28 | 5.42 |
| $WTe_2$ $\chi$ | 3.93 | 4.47 |
| $WTe_2$ $IE$ | 4.98 | 5.20 |

We calculated the electron affinity and ionization energy of single-layer TMDCs with 4% tensile strain. The electron affinity and ionization energy are defined as the energy difference between CBm and vacuum level and the energy difference between vacuum level and VBM. The trends of CBm and VBM with tensile strains are shown in Fig. S3, and the numeric values of $\chi$ and $IE$ are listed in Table S1. We finds that (i) The CBms of all these 2D semiconductors decreased with tensile strain. (ii) the VBM of $MoS_2$ and $WS_2$ increased with 4% tensile strain while the VBM of $MoSe_2$, $WSe_2$, $MoTe_2$, and $WTe_2$ reduced.

The reason for this variation can be attributed to the bonding type of CBm and VBM in monolayer TMDCs. It has been proved by Shi *et al*, in monolayer $MoS_2$, the VBM states mainly originate from Mo $d_{xy}$-like bonding with S ($p_x$+$p_y$), and the CBm is mainly contributed by Mo $d_{z2}$ antibonding with S ($p_x$+$p_y$) obitals (shown in Fig. 6).[1] The biaxial in-plane strain we discussed is along a, b directions in the x, y plane shown in Fig. 1 in the main text. For $MoS_2$, with increasing in-plane tensile strain, the interlayer distance decreases, which leads to the energy of CBm band (in reference to the vacuum level) decrease continuously due to its antibonding character. While the energies of VBM band increase, because of the bonding characters along the x, y directions.

The type of SB is important since the reduction of n-type SBH is determined by the decrease of CBm, while the reduction of p-type SBH should be attributed to the increase of VBM. The contact type is determined by the relative positions of CBm, and VBM of TMDCs and the $E_F$ in TMDCs/metals which mainly relate to the nature of the electron affinity and ionization energies of monolayer TMDCs and the work functions of metal surfaces, respectively. $MoS_2$ has the lowest CBm and VBM, and $WSe_2$ has the highest CBm. These explain why $MoS_2$ is usually n-type in experiments while $WSe_2$ is p-type at most of time. Compared with $MoS_2$, $WSe_2$ has higher CBm and VBM and therefore has higher electrons barrier height but lower holes barrier height for given metals, resulting in easier hole injection but more difficult electron injection.[2]

In addition to $MoS_2$ and $WSe_2$, the contact types of $MoSe_2$/metal, $WS_2$/metal, $MoTe_2$/metal, and $WTe_2$/metal may be between n-type and p-type. The type depends on the work function of different metal surfaces. For $MoTe_2$, the devices combined by $MoTe_2$ and metal surfaces display strong p-type and weak n-type properties.[3] For $MoSe_2$, n type will be formed with low work function metals, such as Er, Mg, Al, Cd, Ag, Sc, Ti, Zr, Hf, and Ir; while p type will be formed with relative high work function metals, such as Pt, Pd, Au, and so on.[4]

For $MoS_2$/metals n-type contacts, values of Schottky barriers height accord with Equation 4, modified n-type Schottky-Mott model in main text. The reduction of SBH with tensile strain is largely attributed to the decrease of $MoS_2$ electronic affinity. In Fig. S3, the CBm energies of $MoS_2$ and $MoSe_2$ decrease with tensile strain, which indicates the n-type SBH in $MoS_2$/metal and $MoSe_2$/metal will decrease with tensile strain.

For p-type contacts, $MoTe_2$/metal and $WSe_2$/metal, the Schottky barrier accord with Equation S3, modified p-type Schottky-Mott model. Similar to n-type contacts, the reduction of p-type SBH largely based on ionization energy. According to the Equation S3, the p-type SBH will decrease when the VBM of $MoTe_2$ and $WSe_2$ increase relative to the vacuum energy. In order to rise up the anti-bonding VBM, compressive strain may be needed.

## Section 4. Single-layer $MoS_2$/Ti and double-layers $MoS_2$/Ti

Table S2. Optimized interlayer distances ($D_{S-M}$), tunneling barrier height (TBH), and tunneling probability (TP) of monolayer $MoS_2$/Ti contacts under strains varied from -2% to 6%.

| Strain | -2% | 0% | 2% | 4% | 6% |
|---|---|---|---|---|---|
| $D_{S-M}$(Å) | 1.62 | 1.58 | 1.55 | 1.51 | 1.48 |
| TBH (eV) | 0 | 0 | 0 | 0 | 0 |
| TP (%) | 100 | 100 | 100 | 100 | 100 |

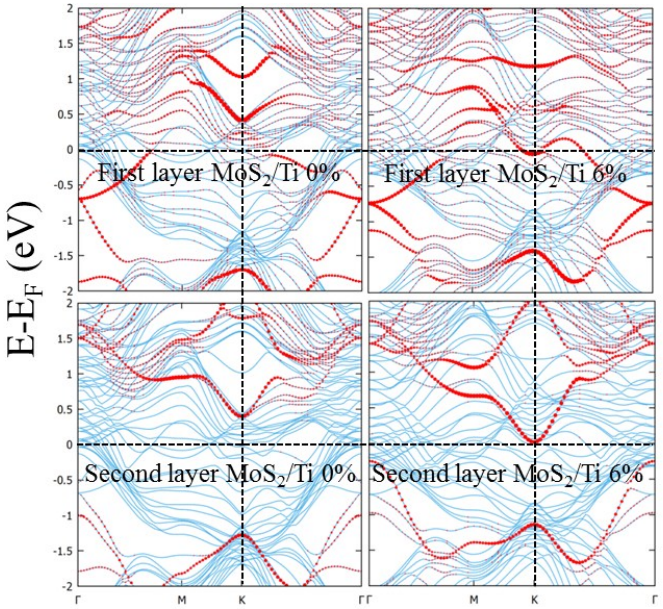


Fig. S4. Band structures of the first and second layer of double-layer $MoS_2$ under strain in contacts to Ti (0001) surfaces. The blue curves are the overall band structures. The red dots represent the projection of Mo *d*-orbitals with its weight represented by the dot size. The Fermi level is set at E=0 eV, shown by the black dotted line.

We also study both SB and TB of $MoS_2$ with Ti (0001) surfaces. We choose $1 \times 1$ $MoS_2$ to match 1×1 Ti (0001) surface, and six layers of Ti atoms are used to model the metal electrodes. We first study single-layer $MoS_2$/Ti, the interaction between $MoS_2$ and Ti are so strong that the TBH keep *zero* during the various strain shown in Table S2. Therefore, double-layer $MoS_2$/Ti should be considered,[5] and the projected band structures of double-layer $MoS_2$/Ti (0001) surfaces with strains are shown in Fig. S4. Since chemical bonds are formed between interlayer S and Ti atoms, the band structure of metallic $MoS_2$ (first layer) hybrid at Fermi level with metal Ti, thus generates *zero* SBH,

and the SB formed between second layer $MoS_2$ and first $MoS_2$. The SB in double-layer $MoS_2$/Ti keeps as n-type during the strains range from 0% to 6%, and the values of SBH almost linearly reduced from 0.41 eV to 0 eV.

## References:


1. H. Shi, H. Pan, Y.-W. Zhang and B. I. Yakobson, *Physical Review B*, 2013, 87, 155304.
2. Y. Liu, P. Stradins and S.-H. Wei, *Science Advances*, 2016, 2, 1600069.
3. C. Kim, I. Moon, D. Lee, M. S. Choi, F. Ahmed, S. Nam, Y. Cho, H.-J. Shin, S. Park and W. J. Yoo, *ACS Nano*, 2017, 11, 1588-1596.
4. L. Huang, B. Li, M. Zhong, Z. Wei and J. Li, *The Journal of Physical Chemistry C*, 2017, 121, 9305-9311.
5. M. Farmanbar and G. Brocks, *Physical Review B*, 2016, 93, 085304.